NANO LETTERS

Letter

pubs.acs.org/NanoLett

Charge Blinking Statistics of Semiconductor Nanocrystals Revealed by Carbon Nanotube Single Charge Sensors

Ewa Zbydniewska,[†,‡] Anna Duzynska,[‡] Michka Popoff,[†,¶] Djamila Hourlier,[†] Stéphane Lenfant,[†] Jaroslaw Judek,[‡] Mariusz Zdrojek,[‡] and Thierry Mélin*[,†]

[†]Institute of Electronics Microelectronics and Nanotechnology, IEMN-CNRS UMR 8520, Avenue Poincaré CS60069, 59652 Villeneuve d'Ascq France

[‡]Faculty of Physics, Warsaw University of Technology, Koszykowa 75, 00-662 Warsaw, Poland

[¶]Lille Centre for Infection and Immunity, Cellular Microbiology of Infectious Pathogens, CNRS UMR8204, INSERM U1019, University of Lille Nord-de-France, Institut Pasteur de Lille, F-59019 Lille, France

Supporting Information

ABSTRACT: We demonstrate the relation between the optical blinking of colloidal semiconductor nanocrystals (NCs) and their electrical charge blinking for which we provide the first experimental observation of power-law statistics. To show this, we harness the performance of CdSe/ZnS NCs coupled with carbon nanotube field-effect transistors (CNTFETs), which act as single charge-sensitive electrometers with submillisecond time resolution, at room temperature. A random telegraph signal (RTS) associated with the NC single-trap charging is observed and exhibits power-law temporal statistics ($\tau^{-\alpha}$, with α in the range of ~1−3), and a Lorentzian current noise power spectrum with a well-defined $1/f^2$ corner. The spectroscopic analysis of the NC−CNTFET devices is consistent with the charging of NC defect states with a charging energy of $E_c \geq 200$ meV. These results pave the way for a deeper understanding of the physics and technology of nanocrystal-based optoelectronic devices.

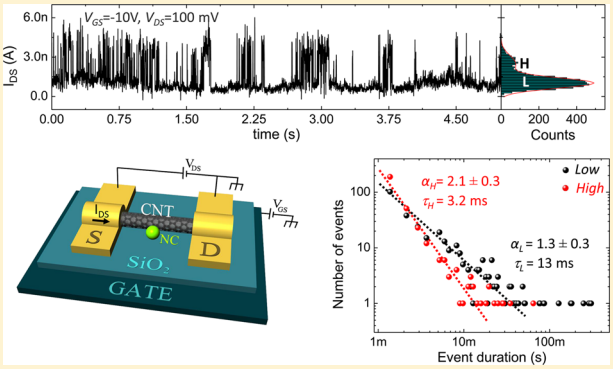

KEYWORDS: *Carbon nanotube field effect transistor, room-temperature single charge sensing, colloidal nanocrystals, charge blinking, random telegraph noise, band gap defects*

Optical blinking of semiconductor nanocrystals (NCs) is one of the most fascinating observations of a two-state system intermittency in which the light emission from a nanocrystal is switched on and off by the fluctuation of the charge occupation of a single electronic state.[1] Early evidence has indicated photoluminescence blinking at a time scale of ~1 s in cadmium selenide nanocrystals.[2] A charging model based on NC photoionization has been proposed, whereas the related on/off charge state intermittency has been directly demonstrated at low blinking frequencies using electrostatic force microscopy on individual nanocrystals.[3] However, more recent work has shown that the physics associated with optical blinking is more complex.[1,4,5] In particular, a second type of blinking, called B-type blinking, has been identified;[1] this type of blinking exhibits typical power-law behavior for the photoluminescence on/off dynamics on the 10 ms to 10 s time scale with unchanged photoluminescence lifetime during the on or off periods. Optical blinking has been attributed to the intermittent occupancy of recombination centers (trap states) in the NC band gap. However, no link has yet been experimentally established between the power-law dynamics observed in fluorescence experiments and the actual dynamics of the NC electrostatic charge population.

In this Letter, we investigate the charge fluctuation dynamics of individual CdSe/ZnS semiconductor NCs using CNTFETs as single charge sensors. CNTFET devices have already been investigated at low temperature to demonstrate and detect single charging events in metallic NCs[6,7] and to probe the charging spectrum of semiconductor NCs.[8] In addition, they have also been used as few-electron/single-electron charge sensors at room temperature in ambient air[9] and, very recently, in a liquid environment.[10] In the present work, to study the charge fluctuation dynamics of individual semiconductor NCs we probed individual semiconductor NCs attached to CNTFETs with a submicrosecond time resolution and with single-charge sensitivity at room temperature. Electrical blinking manifests as a pronounced random telegraph signal (RTS) associated with upper and lower current levels through the CNTFET devices. The RTS analysis shows clear power-law

Received: April 7, 2015
Revised: September 25, 2015
Published: September 29, 2015

DOI: 10.1021/acs.nanolett.5b01338
Nano Lett. 2015, 15, 6349−6356

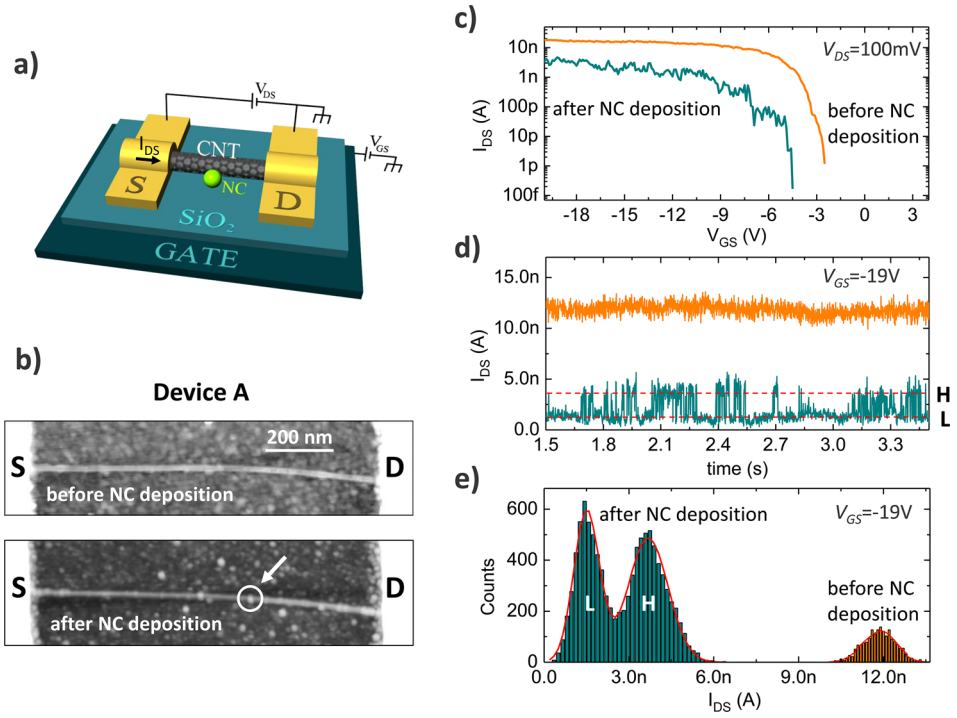

Figure 1. Device A random telegraph signal. (a) Schematics of CNTFETs fabricated on an SiO_2 layer grown on a doped silicon wafer acting as a back-gate. A bias V_{DS} is applied between the source (S) and drain (D) contacts. The current through the nanotube I_{DS} is probed as a function of the back-gate bias V_{GS}. An NC is sketched along the CNTFET channel. (b) Atomic force microscopy topography images of Device A, which was fabricated from a semiconducting nanotube grown by chemical vapor deposition on a 1 μm thick SiO_2 layer, before and after NC deposition (here, 4 nm outer diameter CdSe/ZnS NCs, see text). The topography image z-scale was set to 15 nm to enhance the topographic features in the vicinity of the CNTFET channel. The source and drain contacts therefore correspond to the saturated S and D white areas in the topography images. A single NC added via the deposition process is identified along the CNTFET; the NC exhibits a recorded height of 4 nm. (c) Transfer characteristics $I_{DS}(V_{GS})$ of the CNTFET before (orange) and after (blue) NC deposition. (d) Current time trace $I_{DS}(t)$, as recorded at fixed V_{GS}, before (orange) and after (blue) NC deposition. The NC deposition induced a pronounced intermittency between the two current levels labeled H and L. (e) Corresponding current histograms before and after NC deposition. The current histogram probed before NC deposition is also shown for sake of comparison.

temporal statistics of upper and lower current states (i.e., statistics varying as $\tau^{-\alpha}$ with α in the ~1−3 range) and a Lorentzian current noise power spectrum. The spectroscopic analysis of the coupled NC-CNTFET devices shows that the electrical blinking is due to the charging of the NC defect states with a measured charging energy of $E_c \geq 200$ meV. This origin of the electrical blinking suggests that the power-law statistics of optical blinking is governed by the population statistics of the underlying NC trap states.

Samples were fabricated using standard nanofabrication techniques (see Supporting Information). We worked both with (i) single-walled carbon nanotubes directly grown by chemical vapor deposition on oxidized silicon substrates and with (ii) commercial semiconducting nanotubes (99% pure semiconducting single-walled carbon nanotubes, NanoIntegris). Atomic force microscopy (AFM) images and electrical characteristics of the CNTFETs were systematically measured prior to and after deposition of semiconducting nanocrystals to ensure the deposition of individual semiconducting NCs along the CNTFET channels. To guarantee that the observed power-law electrical blinking statistics did not depend on the CNTFET device fabrication, we also studied two types of devices, labeled Device A and Device B hereafter, which were fabricated using two different approaches. Device A consisted of a CNTFET constructed from single-walled nanotubes grown by chemical vapor deposition on a 1 μm thick SiO_2 layer thermally grown from a p-type degenerately doped silicon wafer. Source and drain contacts were deposited by Ti (5 nm)/Au (45 nm) metal evaporation, and a CNTFET channel of ~1 μm length was defined. CdSe/ZnS NCs with 4 nm outer diameter (purchased from MKNano) were subsequently deposited by being drop-cast onto the fabricated CNTFET. Device B consisted of a CNTFET constructed from commercial semiconducting nanotubes (purchased from Nano-Integris) deposited from a dichloromethane suspension onto a thermally oxidized silicon wafer. This device exhibits a geometry similar to that of Device A, except for the difference in the SiO_2 thickness (300 nm thick thermal dioxide) and the deposited NC size (CdSe/ZnS NCs with measured 5 nm outer diameter, purchased from MKNano).

The devices (including the CNTFET wiring) are sketched in Figure 1a. AFM images of Device A before and after NC deposition are provided in Figure 1b. The comparison between the two AFM images shows the presence of an isolated NC adsorbed along the CNTFET channel, as a result of the NC deposition process (see the white arrow as a guide to the eye).[11] The electrical characteristics $I_{DS}(V_{GS})$ of Device A before and after NC deposition are shown in Figure 1c. Unlike previously published experiments at low temperature,[7,8] which reveal a series of individual jumps in the $I_{DS}(V_{GS})$ characteristics ("hole per hole"charging of the NC during the back-gate bias sweep), such jumps are not clearly observed here. This lack of observed jumps is a consequence of our devices operating at room temperature and in ambient air, whereas previous

DOI: 10.1021/acs.nanolett.5b01338
Nano Lett. 2015, 15, 6349−6356

experiments have been performed at temperatures much smaller than the dot interlevel spacing (i.e., for $k_BT \ll \Delta E$, in which $\Delta E \approx 25-50$ meV[8] accounts for the electrostatic and quantum confinement energies) and were performed in vacuum. The main feature observable in the electrical characteristics is a "flattening" of the $I_{DS}(V_{GS})$ curve after a NC is attached to the device (i.e., a gradual decrease of the current level with increased negative back-gate bias V_{GS}), as shown in Figure 1c. This feature is typical of coupled NC-CNTFET devices and is the global result of charge transfer from the CNTFET to its environment upon the application of a back-gate after NC deposition.[8] An increased noise (Figure 1c) is also visible in the $I_{DS}(V_{GS})$ characteristics after NC deposition compared to the characteristics prior to NC deposition. To isolate this effect, current versus time $I_{DS}(t)$ data were recorded at fixed V_{GS} and are shown in Figure 1d. The data clearly show that the NC induces a pronounced random telegraph noise in the CNTFET current, where higher (H) and lower (L) current levels (with mean values of 3.6 and 1.5 nA, respectively) can unambiguously be identified at fixed gate bias. The two-level intermittency between the H and L levels corresponds to the semiconductor NC carrying N and N + 1 charges and is unambiguously revealed by the histogram of the current levels in the $I_{DS}(t)$ data, as shown in Figure 1e. This RTS signal can be used to study the "electrical blinking" of the NCs using the CNTFETs as charge detectors.

A similar behavior is observed for Device B, as shown in Figure 2. Device B topography is shown in Figure 2a, where the circled area corresponds to a NC (measured height ~5 nm) identified after the deposition of CdSe/ZnS NCs. The transfer characteristics $I_{DS}(V_{GS})$ of the device before and after NC deposition are shown in Figure 2b for a source-drain bias V_{DS} = 150 mV. A very similar flattening effect in the $I_{DS}(V_{GS})$ is observed compared to that observed for Device A. We also recorded the back-and-forth back-gate bias sweeps for the $I_{DS}(V_{GS})$, showing an increased hysteresis in the presence of the NC along the CNTFET channel. This effect is not expected from a purely reversible NC charging effect but may be due to charge exchange processes with slow time-scale dynamics at the NC/SiO_2 substrate interface[12] upon changes in the gate bias V_{GS}. Current time traces $I_{DS}(t)$, shown in Figure 2c after the NC deposition (V_{DS} = 150 mV, V_{GS} = −8 V) display a pronounced RTS after the NC deposition, similar to Device A, with L and H current levels of 0.8 and 1.5 nA, respectively. The corresponding histogram is shown in Figure 2d, which shows an asymmetry between the occupation of the two levels.

To gain insight into the statistics of the charge jumps, we measured the $I_{DS}(t)$ time traces of the devices using a recording bin time of τ_{min} = 1 ms and a total integration time of τ_{max} = 5 s for Device A and τ_{min} = 0.1 ms and τ_{max} = 1 s for Device B to explore NC charging dynamics on shorter time scales. An example of raw experimental $I_{DS}(t)$ traces are shown in Figure 3a,d. Idealized time traces were also computed (data not shown), where the introduction of a threshold enables the transformation of the experimental $I_{DS}(t)$ traces into a pure RTS signal between L and H levels with amplitudes 0 and 1, respectively. From the idealized time traces, we derive the statistics of the levels L and H, which are plotted as a function of the event duration in Figure 3b,e. This plot shows a clear power-law behavior for the NC charging events (probabilities $P_{L,H}(\tau)$ for the high/low events proportional to $\tau_{L,H}^{-\alpha_{L,H}}$). The associated measured exponents are α_L = 1.3 ± 0.3, α_H = 2.1 ± 0.3 (Device A), and α_L = 3.1 ± 0.4, α_H = 1.3 ± 0.4 (Device B).

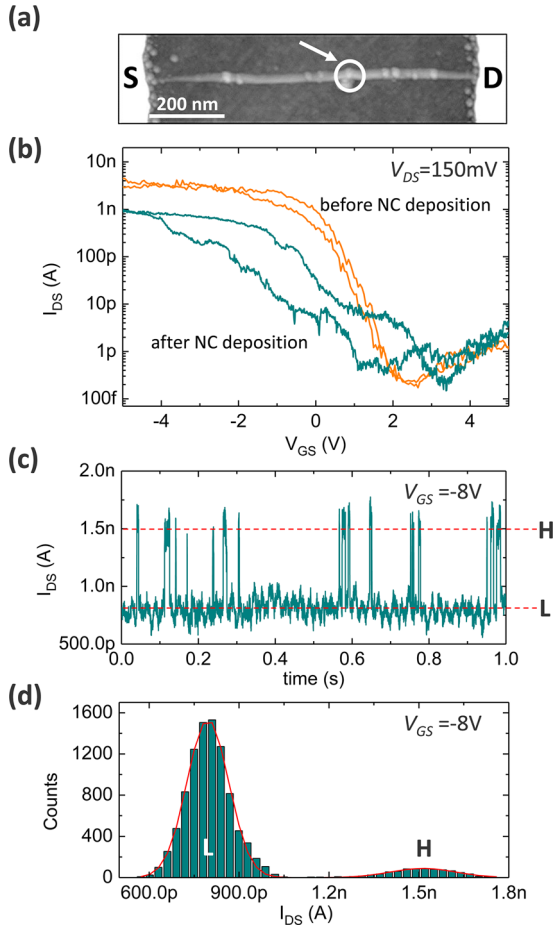

Figure 2. Device B random telegraph signal. (a) Atomic force microscopy image of Device B after the deposition of CdSe/ZnS NCs (see text). The highlighted feature corresponds to a NC (height 5 nm) identified after the deposition process. The image z-scale is 15 nm. (b) Transfer characteristics $I_{DS}(V_{GS})$ of the CNTFET (here, under dry atmosphere) before (orange) and after (blue) NC deposition, using V_{DS} = 150 mV. The hysteresis upper branches correspond to gate bias sweeps toward negative V_{GS}. (c) Current signal plotted as a function of time I_{DS} (t) at fixed V_{GS} = −8 V after NC deposition; the signal shows two current levels (L and H). The graph also contains a parasitic current oscillation at 50 Hz. (d) Current histograms after the NC deposition, corresponding to the graph of $I_{DS}(t)$ shown in (c).

The average times spent on the levels L and H are provided in Figure 3b,e but will not be further analyzed because they depend on the bin time τ_{min} and total integration time τ_{max} for a power-law behavior. The α values may also depend to a smaller extent on τ_{min} and τ_{max}. These effects have previously been studied.[13−16] However, our purpose here is to clearly demonstrate the existence of power-law behaviors in the charging dynamics of NCs, as shown in Figure 3b,e, rather than to provide a refined measurement of the α coefficients.

Furthermore, we computed the power spectrum noise (in A^2/Hz) from the $I_{DS}(t)$ time traces for Devices A and B, which are shown in Figure 3c,f. This approach is common in characterizations of the RTS arising in field-effect transistors with small (sub-μm) dimensions[17,18] as well as for RTS in CNTFETs at low temperatures.[19] It has also been used to characterize the power-law exponents at hand in optical blinking experiments.[20] Here, we observe for both samples a clear Lorentzian shape for the current trace power spectrum, that is, a saturation plateau below the corner frequency f_c and a

DOI: 10.1021/acs.nanolett.5b01338
Nano Lett. 2015, 15, 6349−6356

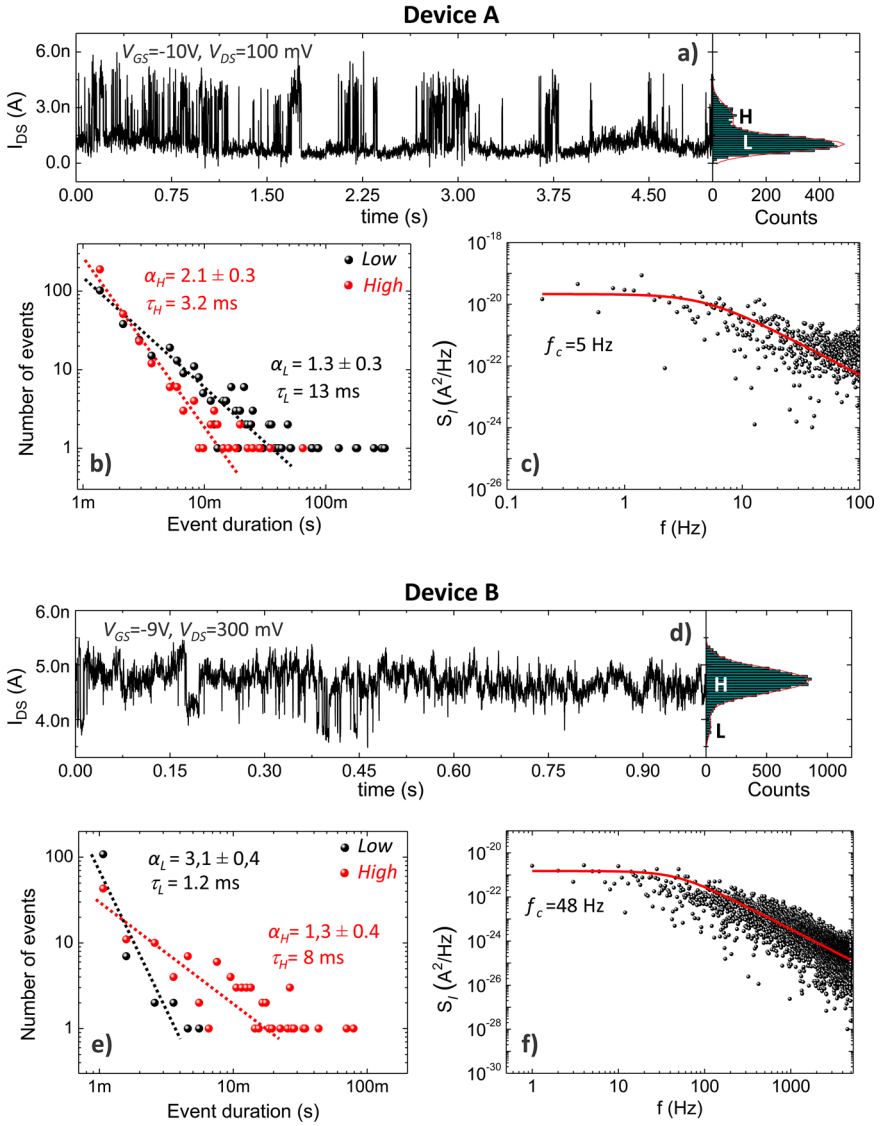

Figure 3. Power-law temporal statistics. Statistical analysis of the RTS noise for Device A (top) and Device B (bottom). (a,d) Experimental time traces of the current I_{DS}, as recorded at fixed gate bias (V_{GS} = −19 V and V_{GS} = −10 V for Devices A and B, respectively). Current histograms are provided to show the separation between the L and H levels. The time bin and integration times are τ_{min} = 1 ms and τ_{max} = 5 s (Device A) and τ_{min} = 0.1 ms and τ_{max} = 1 s (Device B), respectively. (b,e) Statistical analysis of the time spent in the L and H levels; the analysis indicates power-law behaviors (see text). (c,f) Power spectra of the experimental $I_{DS}(t)$ time traces, showing Lorentzian shapes with well-defined corner frequencies f_c and $1/f^2$ slopes (the red lines are Lorentzian fits to the experimental data).

$1/f^2$ slope (slope −2 in the logarithmic representation of Figure 3c,f). We extract from these graphs the RTS corner frequency f_c from a Lorentzian fit to the current trace power spectrum. This yields f_c = 5 Hz for Device A and f_c = 48 Hz for Device B. The corner frequencies differ significantly, but they are also related to the average times $\langle\tau_{L,H}\rangle$ spent on each of the levels L and H and therefore depend both on $\alpha_{L,H}$ and on the choice of the bin time τ_{min} and maximum integration times τ_{max}.[13−16] However, the observation of such a clear Lorentzian spectrum from electrical experiments is striking compared, for example, to nanowire field-effect transistor devices with an RTS caused by a few oxide traps[18] for which the Lorentzian shape of the RTS power spectrum appears as a deviation from or a shoulder to the dominant $1/f$ background noise. We associate this effect with the large amplitude of the RTS observed in our experiments (up to a factor of 2 between the L and H current levels) compared to the work of ref 18 (i.e., less than 10% difference between the L and H current levels, at most).

The observation of a power-law behavior is consistent with the optical blinking of similar CdSe NCs capped with ZnS, as observed from fluorescence experiments,[13] or for different colloidal NCs.[1,14,20] We experimentally verified that the NCs used in this work exhibited fluorescence blinking (see the Supporting Information) either on insulators or when deposited onto a dense carbon nanotube layer.[21] Notably, however, electrical blinking in our work was observed in the dark. Only the NC electrostatic charge state is indeed probed here in the absence of optical excitation, which separates electrostatic issues from the optical processes associated with NC blinking.[1] To our knowledge, these experiments are the first demonstration of electrostatic experiments in which a power-law statistical distribution of the NC charge state is observed. Indeed, pioneering work probing single charge

DOI: 10.1021/acs.nanolett.5b01338
Nano Lett. 2015, 15, 6349−6356

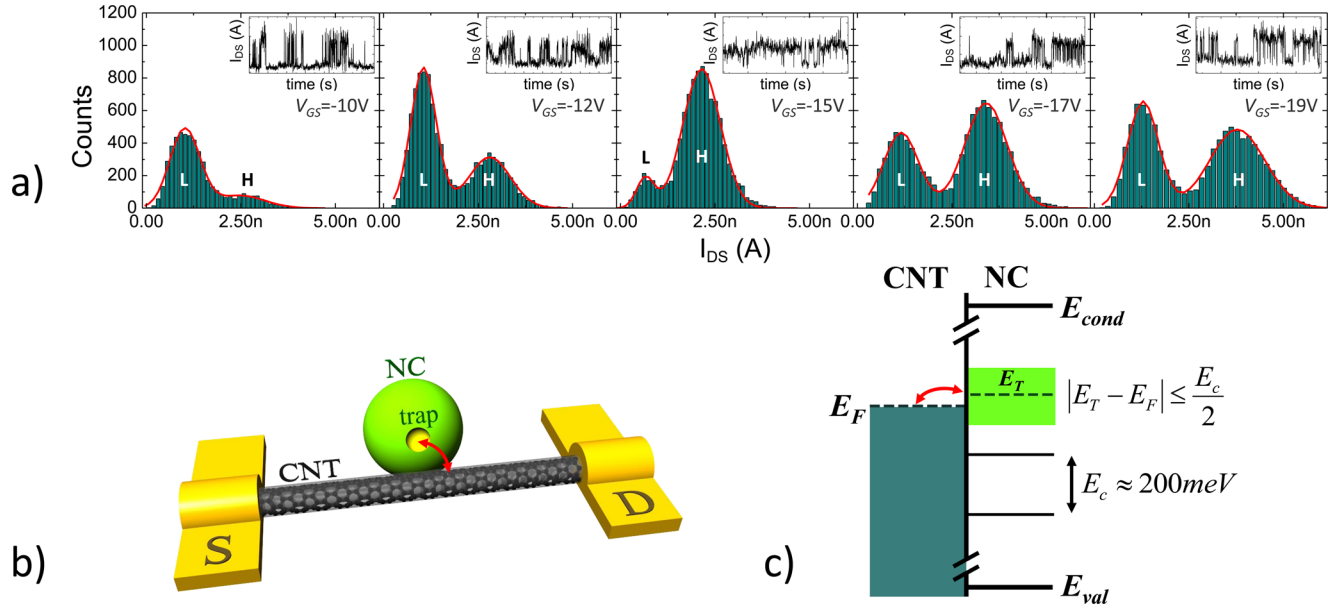

Figure 4. RTS back-gate dependence for Device A. (a) Histograms of I_{DS} current levels recorded as a function of the back-gate bias V_{GS}. The device current was recorded for each plot using a recording bin time τ_{min} = 10 ms. The total recording time was τ_{max} = 5 s (V_{GS} = −10 V) or τ_{max} = 10 s (V_{GS} = −12 V to −19 V). Insets show the RTS of the current traces. (b) Schematics of the charge transfer between the CNTFET and the NC trap. (c) Energy diagram showing charge transfers between the CNTFET (treated as a metal electrode) and NC band gap traps with charging energy E_c. E_{cond} and E_{val} refer to the NC conduction and valence bands, respectively. In this picture, we only take into account the trap electrostatic charging energy E_c by assuming that the energy difference between trap levels ΔE_T stays small as compared to E_c ($\Delta E_T \ll E_c$, see text).

fluctuations of CdSe NCs by electrostatic force microscopy[3] suffered from intrinsic bandwidth limitations and could not reveal NC blinking statistics. Previous experiments based on single charge detection using CNTFETs were neither focused on NC blinking nor on the statistical aspects of charge fluctuations.[8,10] Finally, recent work has focused on current blinking in the transport through colloidal dots, either from transport measurements using static electrodes[22] in the case of CdSe/CdS NCs or using conductive AFM in the case of PbS or PbSe dots.[23] Such measurements revealed ON and OFF current states with power-law statistics or a Lorentzian power spectrum but did not demonstrate experimentally the fluctuation statistics of the single charge state involved in their interpretation.

To further assess the physical mechanisms associated with the NC electrostatic blinking, we performed a spectroscopic analysis of the devices to measure the charging energy E_c associated with the RTS. In Figure 4, we show the RTS properties of Device A probed as a function of the CNTFET back-gate, which is varied by ΔV_{GS} steps of 2 or 3 V. Such large ΔV_{GS} steps were chosen to explore the full V_{GS} range of the device in which the RTS could be observed (see the discussion hereafter). The observed RTS histograms are presented in Figure 4a (the insets illustrate the associated current jump events over a reduced time range) for V_{GS} values where the RTS could be observed. We verified that the RTS could not be identified beyond the V_{GS} range of Figure 4 in the recording conditions. Figure 4a shows that the RTS definitely varied upon changes to the back-gate bias, although a monotonous trend for the relative histogram weights of the L and H current levels was not observed. This effect likely arises because the steps in ΔV_{GS} induce shifts of the NC electrostatic potential larger than the NC charging energy. This effect can also be explained in part by the fact that the application of a sudden change in V_{GS} can alter the global device gating properties;[7] alternatively, it can be explained by the presence of different trap centers in the charging process for different V_{GS} (see the discussion hereafter).

To estimate the NC charging properties from the RTS data in Figure 4a, we followed the approach used to model the RTS induced by trap states in early sub-μm Si FET devices.[24] This approach relates the ratio between the trap capture and emission times to the trap charging energy. This model describes the statistics of the trap center in equilibrium with the Fermi level of the electronic device channel (see the schematics in Figure 4b). This model can be adapted here to compute the energy difference between the NC electronic state with energy E_T involved in the RTS process, as well as the local Fermi level E_F in the CNTFET, from the average times spent on the L and H current levels

$$\frac{\langle \tau_L \rangle}{\langle \tau_H \rangle} = \exp\left[\frac{E_T - E_F}{k_B T}\right] \quad (1)$$

We used this equation and the average times $\langle \tau_L \rangle$ and $\langle \tau_H \rangle$ derived from the RTS plots in Figure 4 to analyze the variations of $E_T - E_F$ when the back-gate bias V_{GS} was swept in Device A. Results are shown in Table 1. The trap charging energy shows a large dispersion with positive and negative values and a maximum absolute value of $|E_T - E_F|_{max} \approx 70$ meV. To explain these variations, we propose that the RTS is due to the charging of a NC band gap trap with energy E_T in equilibrium with the CNTFET channel (here, in a metallic representation) with local Fermi level E_F. The charging process is illustrated in Figure 4b together with a simplified energy diagram provided in Figure 4c in which we consider that the trap charging energy E_c is much larger than the energy difference ΔE_T between two different traps (this quantity is therefore not represented in Figure 4c). This leads to a simple picture of energy levels organized in the form of a "ladder" separated by E_c ($E_c \gg \Delta E_T$

DOI: 10.1021/acs.nanolett.5b01338
Nano Lett. 2015, 15, 6349−6356

Table 1. Analysis of the RTS in Device A[a]

V_{GS}	$\langle\tau_L\rangle/\langle\tau_H\rangle$	$2(E_T - E_F)$	$\Delta V_{GS}(L-H)$	$e\Delta V_{GS}(L-H)/\beta$
−10 V	16	144 meV	0.80 V	215 meV
−12 V	0.90	−6 meV	0.83 V	225 meV
−15 V	1.8	30 meV	0.8 V	215 meV
−17 V	0.14	−100 meV	1.0 V	270 meV
−19 V	0.47	−38 meV	1.0 V	270 meV

[a]The table shows the operation back-gate bias V_{GS}, the ratio between the average times $\langle\tau_L\rangle$ and $\langle\tau_H\rangle$ (data from Figure 4), the trap energy with respect to the CNTFET Fermi level $E_T - E_F$ (see text), the back-gate voltage difference between the current levels I_L and I_H associated with the L and H states (obtained from the transfer characteristics of Device A without NC), and the corresponding charging energy obtained using the lever arm $\beta = 3.7$ taken from ref 8.

prevents the simultaneous charging of several traps). In this most simple picture, the energy mismatch between E_F and E_T is necessarily limited by $E_c/2$, as shown in Figure 4c. Using the measured value of $|E_T - E_F|_{max} \approx 70$ meV, this yields $E_c \geq 2\,|E_T - E_F|_{max} \approx 140$ meV. Such a value is large compared to the charging energy already observed in the case of metal NCs ($E_c \approx 5$ meV[7]) or to that reported for CdSe NCs of similar size ($E_c \approx 20-40$ meV[8]). It is, however, consistent with the charging of NC band gap trap states and is furthermore in agreement with our observation of two-level RTS at 300 K.

To support this claim, we estimated E_c using an alternative method. We consider for each gate voltage V_{GS} the values of the L and H average current levels, as extracted from the histograms in Figure 4. We then use the CNTFET characteristics of Device A prior to NC deposition to estimate the back gate voltage shift $\Delta V_{GS}(L-H)$ corresponding to the switch between the two current values. Raw values of $\Delta V_{GS}(L-H)$ are presented in Table 1 and exhibit relatively stable values in the range of 0.8−1 V. These values, however, refer to the voltage applied to the CNTFET back-gate, which is related to the real NC electrostatic energy by a lever arm β. This lever arm has been estimated as $\beta = 3.7$ in a previous work[8] for a CNTFET device geometry (i.e., channel length and oxide thickness) similar to that of Device A. We therefore extract the NC charging energy as $e\Delta V_{GS}(L-H)/\beta$, as provided in Table 1. Remarkably, these values are rather constant (in the 215−270 meV range) as a function of V_{GS} and remain above the 140 meV value extracted from the maximum value of $E_T - E_F$ in the RTS analysis. This result is fully consistent with the fact that $E_c \geq 2|E_T - E_F|_{max}$ in the trap-charging RTS model. It is also consistent with the fact that the measured $E_T - E_F$ values shown in Table 1 were randomly observed to be positive or negative, which is a consequence of the fact that the back-gate bias steps applied to the device $e\Delta V_{GS}/\beta$ are larger than E_c.

These results support our model of a two-level RTS associated with the population of NC band gap traps with a charging energy $E_c \approx 200$ meV for Device A. The same methodology has also been applied to Device B (detailed analysis provided in the Supporting Information), which yields a trap charging energy $E_c \approx 225$ meV, which is in good agreement with the value obtained for Device A. The attribution of the RTS to trap states is more generally consistent with the following arguments. First, and in contrast with the NC spectroscopy previously performed using CNTFETs at low temperature,[8] we do not observe single charge events out of a back-gate bias "gap" corresponding to the NC band gap but rather within a given range of V_{GS} values with amplitude of 9 V (Device A) and 3 V (Device B). Both amplitudes, when normalized by the lever arm β, fall within the expected band gap of the CdSe/ZnS NCs derived from the absorption peak at 500 nm (Device A) and 620 nm (Device B). Second, the value of the NC charging energy estimated in our work for the two samples and two methods was observed to be close to 200 meV. This value is large compared to the charging energy associated with NC quantum levels[8] (40−50 meV at most, including quantum confinement and Coulomb effects), which underscores the fact that, in our work, the NC charging is not due to the charging of the NC valence-band quantum levels. Finally, the charging mechanism observed is close to the trap charging observed from scanning-tunnelling spectroscopy experiments on CdSe/ZnS NCs[25] in which a trap charging energy of 65 meV has been observed. Notably, this value has been measured for a NC in the gap between a metal tip and an Au substrate; this metallic environment likely explains the larger trap charging energy in our work in which the NCs were inserted into an electronic device constructed on an insulating layer.

We finally discuss in the following our results on a more general basis and in view of future developments. This covers the aspects of NC trap state spectroscopy and the link of our results with NC blinking experiments. As for the spectroscopy of NC trap states, our electrostatic results indicate that NC trap states are energetically disbributed within the NC band gap, but this analysis should be extended in order to determine the trap actual energy distribution. Hence, we determined in the case of Device A that the RTS associated with traps occurs within a back-gate bias range $\Delta V_G = 9$ V, corresponding to a 2.4 eV NC energy range using the lever arm $\beta = 3.7$ for Device A. This range is remarkably close to the NC band gap as deduced from the NC absorption peak at 500 nm. Our measurements are thus consistent for Device A with a picture in which traps would be energetically distributed over the whole NC band gap (in that case, the NC band edges can also be deduced from the charge spectroscopy). This picture is however different for Device B for which traps are observed on a reduced energy range of $\Delta V_G \approx 3$ V (~1 eV NC energy range using a lever arm $\beta' = 2.95$, see the Supporting Information). This value is smaller than the expected NC band gap, suggesting that traps are localized over a reduced band of energies within the band gap, which is in agreement with typical photoluminescence experiments.[26] One cannot so far position here this band of energy with respect to the NC conduction valence and conduction band edges. One way to circumvent this using CNTFET charge detectors would be to lower the device temperature, as done in previous work,[8] and to probe the onset of single electron jumps associated with the charging of the NC conduction and valence electronic states. Such an analysis is however restricted to low temperatures due to the much reduced charging energies ($E_c \approx 20-40$ meV) associated with these states, which cannot be observed at room temperature. A second aspect would be the determination of the donor or acceptor character of the trap states within the band gap. Here again, further developments are required, since experiments using CNTFET as charge sensors only provide measurement of relative changes in the NC charge state (i.e., detecting jumps between N and $N+1$ elementary charges) but not of its absolute charge state N. This type of identification would be likely possible by coupling CNTFET charge sensing with, for example, charge or potential sensing from scanning-probe microscopy, either by Kelvin probe force microscopy or, similarly, by electrostatic force

DOI: 10.1021/acs.nanolett.5b01338
Nano Lett. 2015, 15, 6349−6356

microscopy. The latter technique has been used originally to probe the blinking of an NC from its charge state compared to an HOPG substrate;[3] the two techniques have been more recently used to probe the electrostatics of CNTFETs in the presence of few electron charge spots at the vicinity of the device channel[9] and could be readily extended to probe coupled CNTFET-NC devices such as those of our work. One would here probe directly the electrostatic potential or charge state of a blinking NC with respect to the CNTFET channel potential and thus provide an intrinsic reference for the NC charge state. It should be noted however that scanning-probe techniques have intrinsic bandwidth limitations, especially while preserving the charge detection sensitivity better than the elementary charge in air at 300 K.[3] This is why we primarily used CNTFETs in our work rather than scanning-probe techniques to enable single charge detection with a submillisecond time resolution to record the NC charge blinking statistics.

Finally, the key point in our experiments beyond spectroscopic issues is the identification of the power-law behavior of the electrostatic charge blinking of NCs. Following the discussion of Marcus et al. in the case of optical blinking, this observation rules out possible charging mechanisms based on a single trap filled at a fixed charge transfer rate, or a static distribution of trap states with a distribution of charge transfer times, because in both cases an exponential statistics would be expected, at least for one of the H and/or L states.[27] The observation of power-law statistics in the NC charge blinking thus favors scenarios based on environmentally induced fluctuations of charge transfer rates or from diffusion-controlled models.[27] The use of a sensitive electrostatic NC-CNTFET device to study blinking effects may help in dissociating between both processes, because it is by essence based on the tunneling of single charges from the CNTFET channel to the NC, and on the other hand sensitive to the electrostatic environment of the CNTFET and of the NC. If fluctuations of charge transfer rates would be induced by changes in the NC electrostatic environment, then this would also be detected from the current level flowing through the CNTFET, while the current level is observed as constant within the measurement accuracy and dynamic range. We therefore speculate that the physics behind the observation of the power-laws in the charge blinking statistics is related to diffusion controlled models in which the trap energy is the parameter exhibiting a random walk and creating the observed power-law statistics.

In conclusion, we have observed the charge blinking behavior of CdSe/ZnS NCs at room temperature on the basis of their coupling with CNTFETs used as single charge-sensitive electrometers. The RTS associated with electrical blinking exhibits characteristics typical of optical blinking, that is, power-law temporal statistics ($\tau^{-\alpha}$, with α in the range of ~1−3) and a Lorentzian current noise power spectrum. We performed a spectroscopic analysis of the coupled NC-CNTFET devices, showing either a thermal activation or an out-of-equilibrium population of NC trap states with a measured charging energy of $E_c \approx 200$ meV, which is attributed to trap states within the NC band gap. This work offers the possibility of more sophisticated studies either at lower temperatures for trap state spectroscopy issues, or by directly combining NC trap state spectroscopy using nanoscale charge detectors and individual NC fluorescence dynamics.

■ ASSOCIATED CONTENT

Supporting Information

The Supporting Information is available free of charge on the ACS Publications website at DOI: 10.1021/acs.nanolett.5b01338.

Additional details about the device fabrication, fluorescence blinking experiments, as well as the determination of the charging energy E_c for Device B. (PDF)

■ AUTHOR INFORMATION

Corresponding Author

*E-mail: thierry.melin@univ-lille1.fr.

Notes

The authors declare no competing financial interest.

■ ACKNOWLEDGMENTS

This work has performed using the facilities of the RENATECH program and of the ExCELSiOR Nanoscience Characterization Center. It was supported in part by the French National Research Agency under Contract No. ANR-11-BS10-0004. M.Z. and E.Z. acknowledge support from the Polish project Lider/11/22/L-2/10/NCBR/2011 and Homing Plus/2010-1/15. We thank D. Deresmes and F. Vaurette for their assistance with AFM and EBL, D. Brunel for discussions, C. Delerue, and R. Swirkowicz for a careful reading of the manuscript, and the BioImaging Center Lille (BICeL) (Université Lille Nord de France) for access to the optical microscope setup.

■ REFERENCES

(1) Galland, C.; Ghosh, Y.; Steinbrück, A.; Sykora, M.; Hollingsworth, J. A.; Klimov, V. I.; Htoon, H. *Nature* **2011**, *479*, 203−207.

(2) Nirmal, M.; Dabbousi, B. O.; Bawendi, M. G.; Macklin, J. J.; Trautman, J. K.; Harris, T. D.; Brus, L. E. *Nature* **1996**, *383*, 802−804.

(3) Krauss, T. D.; Brus, L. E. *Phys. Rev. Lett.* **1999**, *83*, 4840.

(4) Zhao, J.; Nair, G.; Fisher, B. R.; Bawendi, M. G. *Phys. Rev. Lett.* **2010**, *104*, 157403.

(5) Rosen, S.; Schwartz, O.; Oron, D. *Phys. Rev. Lett.* **2010**, *104*, 157404.

(6) Marty, L.; Bonnot, A. M.; Bonhomme, A.; Iaia, A.; Naud, C.; André, E.; Bouchiat, V. *Small* **2006**, *2*, 110−115.

(7) Gruneis, A.; Esplandiu, M. J.; Garcia-Sanchez, D.; Bachtold, A. *Nano Lett.* **2007**, *7*, 3766−3769.

(8) Zdrojek, M.; Esplandiu, M. J.; Barreiro, A.; Bachtold, A. *Phys. Rev. Lett.* **2009**, *102*, 226804.

(9) Brunel, D.; Mayer, A.; Mélin, T. *ACS Nano* **2010**, *4*, 5978−5984.

(10) Sharf, T.; Wang, N. P.; Kevek, J.; Brown, M. A.; Wilson, H.; Heinze, S.; Minot, E. D. *Nano Lett.* **2014**, *14*, 4925−4930.

(11) A careful check shows that observable features along the CNTFET channel after NC deposition either (i) already occur at the very same position along the nanotube in the AFM picture before NC deposition or (ii) have been slightly moved along the nanotube during the drop-casting NC deposition process.

(12) Diesinger, H.; Mélin, T.; Deresmes, D.; Stiévenard, D. *Appl. Phys. Lett.* **2004**, *85*, 3546.

(13) (b) Kuno, M.; Fromm, D. P.; Hamann, H. F.; Gallagher, A.; Nesbitt, D. J. *J. Chem. Phys.* **2000**, *112*, 3117−3120;(b) Kuno, M.; Fromm, D. P.; Hamann, H. F.; Gallagher, A.; Nesbitt, D. J. *J. Chem. Phys.* **2001**, *115*, 1028−1040.

(14) Kuno, M.; Fromm, D. P.; Hamann, H. F.; Gallagher, A.; Nesbitt, D. J.; Micic, O. I.; Nozik, A. J. *Nano Lett.* **2001**, *1*, 557−564.

(15) Crouch, C. H.; Sauter, O.; Wu, X.; Purcell, R.; Querner, C.; Drndic, M.; Pelton, M. *Nano Lett.* **2010**, *10*, 1692−1698.

DOI: 10.1021/acs.nanolett.5b01338
Nano Lett. 2015, 15, 6349−6356

(16) Houel, J.; Doan, Q. T.; Cajgfinger, T.; Ledoux, G.; Amans, D.; Aubret, A.; Dominjon, A.; Ferriol, S.; Barbier, R.; Nasilowski, M.; Lhuillier, E.; Dubertret, B.; Dujardin, C.; Kulzer, F. *ACS Nano* **2015**, *9*, 886−893.
(17) See, for example, Uren, M. J.; Kirton, M. J.; Collins, S. *Phys. Rev. B: Condens. Matter Mater. Phys.* **1988**, *37*, 8346. and references therein.
(18) Clément, N.; Nishiguchi, K.; Fujiwara, A.; Vuillaume, D. *Nat. Commun.* **2010**, *1*, 92.
(19) Liu, F.; Wang, K. L. *Nano Lett.* **2008**, *8*, 147−151.
(20) See, for example, Pelton, M.; Grier, D. G.; Guyot-Sionnest, P. *Appl. Phys. Lett.* **2004**, *85*, 819.
(21) Duzynska, A.; Judek, J.; Zdrojek, M. *Appl. Phys. Lett.* **2014**, *105*, 213105.
(22) Lachance-Quirion, D.; Tremblay, S.; Lamarre, S. A.; Méthot, V.; Gingras, D.; Camirand Lemyre, J.; Pioro-Ladrière, M.; Allen, C. *Nano Lett.* **2014**, *14*, 882−887.
(23) Maturova, K.; Nanayakkara, S. U.; Luther, J. M.; van de Lagemaat, J. *Nano Lett.* **2013**, *13*, 2338−2345.
(24) See, for example, Ralls, K. S.; Skocpol, W. J.; Jackel, L. D.; Howard, R. E.; Fetter, L. A.; Epworth, R. W.; Tennant, D. M. *Phys. Rev. Lett.* **1984**, *52*, 228.
(25) Hummon, M. R.; Stollenwerk, A. J.; Narayanamurti, V.; Anikeeva, P. O.; Panzer, M. J.; Wood, V.; Bulovic, V. *Phys. Rev. B: Condens. Matter Mater. Phys.* **2010**, *81*, 115439.
(26) Mooney, J.; Krause, M. M.; Saari, J. I.; Kambhampati, P. *Phys. Rev. B: Condens. Matter Mater. Phys.* **2013**, *87*, 081201.
(27) See, for example, Pelton, M.; Smith, G.; Scherer, N. F.; Marcus, R. A. *Proc. Natl. Acad. Sci. U. S. A.* **2007**, *104*, 14249−14254.

DOI: 10.1021/acs.nanolett.5b01338
Nano Lett. 2015, 15, 6349−6356